G3139 (Oblimersen) may inhibit prostate cancer cell growth in a partially bis-CpG-dependent non-antisense manner

Johnathan C. Lai,[1,3] Luba Benimetskaya,[1] Regina M. Santella,[4] Qiao Wang,[4] Paul S. Miller,[5] and C. A. Stein[1,2]

Departments of [1]Medicine, [2]Pharmacology, and [3]Biomedical Engineering, and [4]Mailman School of Public Health, Columbia University, New York, NY; and [5]Department of Biochemistry and Molecular Biology, Bloomberg School of Public Health, Johns Hopkins University, Baltimore, MD

Abstract

G3139 is an 18-mer phosphorothioate oligodeoxyribonucleotide, which is targeted to the initiation codon region of the *bcl*-2 mRNA. Although treatment of PC3 prostate cancer cells with G3139, which contains two CpG motifs, causes a dramatic decrease in *bcl*-2 protein expression after 3 days, it did not result in significant cellular apoptosis, as it does in many other cell lines. The absence of apoptosis was demonstrated by the absence of pro-caspase 3 cleavage products and of Annexin V cell surface expression. In addition, ATP production and the mitochondrial membrane potential $\Delta\Psi_m$ were preserved. Despite this, G3139 significantly inhibited the rate of cellular proliferation in complete media and blocked cloning in soft agar. G4232, a variant of G3139 that down-regulates *bcl*-2 expression to the same extent but has both CpG cytidines C5 methylated, was only minimally antiproliferative. A series of mismatched G3139-related oligomers were synthesized that could also substantially down-regulate *bcl*-2 protein expression, but only if the CpG motifs were preserved, demonstrating the presence of additional non-antisense mechanisms. G3139 caused production of reactive oxygen species in growth-arrested cells and oxidation of nuclear guanosine to 8-hydroxy-2′-deoxyguanosine, as determined by 1F7 monoclonal antibody staining. Bromodeoxyuridine incorporation studies demonstrated that G3139 induced a G_1-S entry block and an intra-S-phase block in PC3 cells that persisted as long as 3 days. This finding coincides with the observation that expression of several proteins encoded by S-phase genes, including c-*myb* and poly(ADP-ribose) polymerase, were significantly reduced. These results illustrate the complexity of the mechanism of action of G3139 in PC3 cells. (Mol Cancer Ther. 2003;2:1031–1043)

Introduction

Although a plethora of proteins are believed to be involved in the control of cellular apoptosis, members of the *bcl*-2 family are thought to be critical and central regulators. Indeed, an extensive literature has grown around *bcl*-2 (1–3), the founding member of this family, commenting on its strongly pro-life nature. *Bcl*-2 seems to be a predominately integral membrane protein and is found in the outer mitochondrial membrane, endoplasmic reticulum, or outer nuclear membrane (4–7). It is also capable of forming ion channels in artificial membranes (8). At least in part by correcting a defect in ATP/ADP exchange across the mitochondrial membrane (9), *bcl*-2 can block the release of cytochrome *c* into the cytosol. In that location, cytochrome *c* forms an ''apoptosome'' complex with ATP, Apaf-1, and pro-caspase 9, which leads to the cleavage of the latter into an active peptide.

Bcl-2 appears also to function in an antioxidant pathway to prevent apoptosis (10). Stable transfectants of interleukin-3-dependent FL5.12 cells bearing wild-type *bcl*-2 were completely protected from the apoptotic effects of hydrogen peroxide (H_2O_2). This was particularly evident on examination of loss of cellular fluorescence of *cis*-parinaric acid, a naturally occurring lipid that readily incorporates into membranes, where it fluoresces. The presence of reactive oxygen species (ROS) oxidizes the diene moieties present in *cis*-parinaric acid, resulting in loss of fluorescence. However, the process was completely blocked in cells overexpressing *bcl*-2. In addition, *bcl*-2 protected cells from the lethal effects of the oxidizing agent *t*-butyl hydroperoxide (11). Similar results, commenting on the ability of *bcl*-2 to block the generation of ROS, were also obtained by Kane *et al.* (12).

Elevation of *bcl*-2 expression appears to contribute to both *in vitro* and *in vivo* resistance to a large number of anticancer agents, including *cis*-platinum, taxanes, mitoxantrone, Adriamycin, and dexamethasone, and to radiation as well (13–16). High levels and aberrant patterns of *bcl*-2 expression have been noted in a large number of human cancers, including prostate, colorectal, lung, gastric, non-Hodgkin's lymphoma, and myeloma, and both acute and chronic leukemia (2). Attempts to reverse chemoresistance have included down-regulation of *bcl*-2 expression via an antisense RNA strategy. These experiments, performed in MCF-7 cells, rendered them sensitive to Adriamycin (17) and estrogen withdrawal (18). In addition, an adenovirally delivered anti-*bcl*-2 ribozyme induced extensive apoptosis in PC3 prostate cancer cells (19). Indeed, the critical nature of *bcl*-2 in blocking apoptosis seems to be highlighted in a

Received 2/24/03; revised 6/12/03; accepted 7/18/03.

The costs of publication of this article were defrayed in part by the payment of page charges. This article must therefore be hereby marked advertisement in accordance with 18 U.S.C. Section 1734 solely to indicate this fact.

Requests for reprints: C. A. Stein, Albert Einstein Montefiore Cancer Center, Dept. of Oncology, III E. 210 St., Bronx, NY 10467. Phone: (718) 920-8980; Fax: (718) 652-4027. E-mail: cstein@montefiore.org

recent Phase 2 clinical trial of G3139 in advanced melanoma (20, 21), in which impressive response data (in 6 of 14 heavily pretreated patients) were observed when treatment with G3139 was combined with dacarbazine. The compound is currently in late Phase 3 clinical trials for both advanced melanoma and chronic lymphocytic leukemia.

G3139 is an 18-mer phosphorothioate oligodeoxyribonucleotide, which is targeted (*i.e.*, complementary) to the initiation codon region of the *bcl*-2 mRNA (22). The phosphorothioate class of oligomer contains a sulfur atom substituted for oxygen at a nonbridging position at each phosphorus atom in the molecule. First synthesized to be nuclease resistant (although they are by no means nuclease proof), phosphorothioates have been extensively employed as antisense effector molecules for many years (23, 24) because of such favorable properties as retention of the charge and aqueous solubility of the parent phosphodiester oligomer. Nevertheless, despite the apparent success of G3139 at down-regulating *bcl*-2 expression and ostensibly generating a chemosensitive phenotype in several preclinical models, including breast (25), bladder (26), and prostate (27) cancers, additional critical analysis remains necessary. Extreme care is required in data interpretation because of the inherent nonspecificity of phosphorothioate oligonucleotides. This property is engendered, at least in part, by their ability to bind to a large number of proteins, predominately heparin binding proteins [*e.g.*, basic fibroblast growth factor (28)], fibronectin, and laminin (29). Furthermore, we have recently shown, in high passage number PC3 and T24 cells, that G3139, in addition to down-regulating *bcl*-2 expression, also down-regulated the expression of protein kinase C-α but not other protein kinase C isoforms (30). However, this co-down-regulation occurred only at 100-nM G3139 but not at 50-nM G3139, where only *bcl*-2 but not protein kinase C-α expression was diminished. Furthermore, sensitivity to paclitaxel and carboplatin was only observed at 100 nM but not at 50 nM, despite the fact that *bcl*-2 expression was virtually eliminated at both concentrations. These data clearly demonstrated that the down-regulation of *bcl*-2 expression by G3139, as a single event, did not chemosensitize these cells and strongly suggested that other mechanisms were also operative.

In this work, we examine the effects of G3139 treatment of low passage number PC3 cells. We demonstrate that this oligonucleotide is minimally cytotoxic although highly cytostatic. We show that the production of cytostasis in these experiments appears not to heavily depend on *bcl*-2 down-regulation but rather on the presence of the ''bis-CpG'' motif in the G3139 molecule. The presence of this motif leads to an increased block to S-phase entrance (relative to control oligonucleotide treatment) and to the inappropriate production of ROS, leading in turn to DNA oxidation.

Materials and Methods

Cells

Cells were obtained from the American Type Culture Collection (Rockville, MD). PC3 prostate cancer cells were grown in RPMI plus 10% fetal bovine serum, supplemented by 1% nonessential amino acids, 1% pyruvate, 100-units/ml penicillin G sodium, and 100-μg/ml streptomycin sulfate. Stock cultures were maintained at 37°C in a humidified 5% CO_2 incubator. Due to progressive inconsistency in the observed experimental results, PC3 cells were not used after the eighth passage.

Reagents

The anti-*bcl*-2 monoclonal antibody was purchased from DAKO Corp. (Carpinteria, CA). The anti-α-tubulin monoclonal antibody and bromodeoxyuridine (BrdUrd) were from Sigma-Aldrich (St. Louis, MO). The anti-c-*myb* polyclonal, anti-c-*myc* polyclonal, anti-poly(ADP-ribose) polymerase (PARP) monoclonal, anti-lamin polyclonal, anti-cyclin-dependent kinase (cdk) 2 polyclonal, anti-cdk4 polyclonal, and anti-pro-caspase 3 monoclonal antibodies were purchased from Santa Cruz Biotechnology (Santa Cruz, CA). The anti-cyclin D1 monoclonal antibody was purchased from Neo Markers (Union City, CA). Lipofectin was purchased from Invitrogen (Carlsbad, CA). Annexin V-FITC Apoptosis Detection Kit was purchased from BD Biosciences (San Jose, CA). 5,5′,6,6′-tetrachloro-1,1′,3,3′-tetraethyl-benzimidazolcarbocyanine iodide (JC-1), nonyl acridine orange (NAO), 2′,7′-dihydrodichlorofluorescein diacetate (H_2DCF-DA), dihydroethidium (HE), and the ATP Determination Kit were purchased from Molecular Probes (Eugene, OR). Luminescence derived from the luciferin-luciferase reaction in the presence of ATP was measured in a luminometer (Lumat LB9507, EG&G, Berthold, Germany). Noble Agar was purchased from Sigma. Phosphorothioate oligonucleotides were synthesized and purified via standard procedures and kindly supplied by Genta (Berkeley Heights, NJ). A list of the oligomers employed is presented in Table 1.

Oligonucleotide Transfections

Cells were seeded the day before the experiment in six-well plates at a density of 25×10^4 cells/well to be 60–70% confluent on the day of the experiment. All transfections were performed in Opti-MEM medium in the absence of fetal bovine serum (Invitrogen, Grand Island, NY) as per the manufacturer's instructions. The appropriate quantities of reagents were diluted in 100 μl of Opti-MEM medium to give a final concentration of Lipofectin and 400-nM oligonucleotide. The solutions were mixed gently and preincubated at room temperature for 30 min to allow complexes to form. Then, 800 μl of Opti-MEM were added and the solution was mixed and overlaid on the cells that have been prewashed with Opti-MEM. The incubation time for oligonucleotide/Lipofectin complexes in Opti-MEM was 5 h followed by incubation in complete media containing 10% fetal bovine serum (Invitrogen). The total incubation time before cell lysis and protein isolation was usually 72 h at 37°C.

Western Blot Analysis

Cells treated with oligonucleotide-lipid complexes were washed in PBS and then extracted in lysis buffer (50-mM Tris-HCl, pH 7.4, 1% NP40, 0.25% sodium deoxycholate, 150-mM NaCl, 1-mM EGTA, 50-μg/ml Pefabloc SC (Roche,

Table 1. Sequences of phosphorothioate oligonucleotides used

Oligomer	Length	Sequence 5′-3′[a]	Comments
G3139	18	TCTCCCAGCGTGCGCCAT	Two CpG motifs targeted to *bcl*-2 initiation codon
G4216	18	TCTCCCAGC***A***TG***T***GCCAT	G3139 variant with single base mismatch at each CpG motif
2009	20	AATCCTCCCCCAGTTCACCC	No CpG motifs targeted to *bcl*-2 coding region
2006	24	TCGTCGTTTTGTCGTTTTGTCGTT	Triple-tandem repeat optimized human CpG sequences
G4232	18	TCTCCCAG$\overset{*}{C}$GTG$\overset{*}{C}$GCCAT	G3139 variant with cytosine C5 methyl at each CpG motif
G4263	18	TC***C C T***CAGCGTGCGCCAT	G3139 variant with two mismatches neither in CpG motifs
G4264	18	*A*C***C C T***CAGCGGTGCGCCA*C*	G3139 variant with four mismatches, none in CpG motifs
G4273	18	***ATCCTA***AGCGTGCGCC***T***T	G3139 variant with six mismatches, none in CpG motifs
G4274	18	***CTCTAT***AGCGTGCGC***CA***	G3139 variant with eight mismatches, none in CpG motifs
G4275	18	***CTCTATGA***CGTGCG***TACA***	G3139 variant with 12 mismatches, none in CpG motifs
84822	18	TCTCCCAG$\overset{*}{C}$GTGCGCCAT	G3139 variant with cytosine C5 methyl in the 5′ CpG motif
84823	18	TCTCCCAGCGTG$\overset{*}{C}$GCCAT	G3139 variant with cytosine C5 methyl in the 3′ CpG motif
84825	18	TCTC$\overset{*}{C}$CAGCGTGCGC$\overset{*}{C}$AT	G3139 variant with cytosine C5 methyl not present at either CpG motif

[a]Asterisk refers to 5-methyl-deoxycytidine; ***bold italics*** represent mismatched bases.

Indianapolis, IN), 15-μg/ml aprotinin, leupeptin, chymostatin, pepstatin A, 1-mM Na_3VO_4, 1-mM NaF) at 4°C for 1 h. Cell debris was removed by centrifugation at 14,000 × *g* for 20 min at 4°C. Protein concentrations were determined using the Bio-Rad protein assay system (Bio-Rad Laboratories, Richmond, CA). Aliquots of cell extracts, containing 25–50 μg of protein, were resolved by SDS-PAGE and then transferred to Hybond ECL filter paper (Amersham, Arlington Heights, IL), and the filters were incubated at room temperature for 1–2 h in 5% BSA in PBS containing 0.5% Tween 20. The filters were then probed with 1:500 dilutions of the anti-*bcl*-2 antibody in 5% BSA in PBS containing 0.5% Tween 20 at 4°C overnight. After washing in PBS containing 0.5% Tween 20, the filters were incubated for 1 h at room temperature in 5% milk in PBS containing 0.5% Tween 20 with a 1:3000 dilution of a peroxidase-conjugated secondary antibody (Amersham). After washing (3 × 10 min), ECL was performed according to the manufacturer's instructions.

Northern Blot Analysis

Total cellular RNA was isolated using TRIZOL Reagent (Life Technologies, Inc., Naw Nitrogen). Approximately 25–30 μg were resolved on 1.2% agarose gel containing 1.1% formaldehyde and transferred to Hybond-N nylon membranes (Amersham). Human *bcl*-2 probe was ^{32}P-radiolabeled with [α-^{32}P]dCTP by random primer labeling using a commercially available kit (Promega, Madison, WI) according to the manufacturer's instructions. The blots were then hybridized with the cDNA probes in 50% formamide, 5× SSC, 5× Denhardt's solution, 0.5% SDS, and 0.1 mg/ml of salmon sperm DNA overnight at 42°C. The filters were washed at room temperature twice for 15 min in 2× SSC and 0.1% SDS, once for 20 min in 1× SSC and 0.1% SDS, and finally twice for 15 min in 0.1× SSC and 0.1% SDS at 65°C. The filters were exposed to Kodak (Rochester, NY) X-ray film for 12–48 h with intensifying screens at −70°C and then developed.

Determination of Rate of Cell Proliferation in Complete Media

Briefly, 15–20 × 10^4 cells were seeded in six-well plates and allowed to attach overnight. Cells were then treated with the appropriate concentrations of oligonucleotide complexed to Lipofectin (15 μg/ml) for 5 h at 37°C. After 3–7 days of incubation at 37°C, cells were trypsinized and harvested, and their viability was determined by trypan blue exclusion. Experiments were performed in triplicate, and data are presented as averages ± SD. In no experiment did more than 10–15% of cells stain with trypan blue.

Bromodeoxyuridine Incorporation

To evaluate BrdUrd incorporation, cells were treated for 5 h in Opti-MEM with oligonucleotide/Lipofectin complexes and allowed tto incubate in complete media without these complexes for a further 19 or 67 h. Subsequently, the cells were pulsed with 10-μM BrdUrd for 2 h at 37°C in complete media. The media containing BrdUrd was then replaced with complete media. Cells were harvested 0, 4, 8, and 20 h after the BrdUrd pulse. After washing with PBS, the cells were fixed in cold 70% ethanol at −20°C overnight. After washing in PBS, cells were resuspended in 2-N HCl/Triton X-100 at room temperature for 30 min and resuspended in 0.1-M $Na_2B_4O_7$ for 7 min. Then, the cells were treated with an anti-BrdUrd antibody (Becton Dickinson, San Jose, CA) in 0.5% Tween 20/1% BSA/PBS in the dark at room temperature for 45 min and costained with 0.01 mg/ml of propidium iodide (PI) for 30 min. PI and BrdUrd were excited at 488 nm. Ten thousand cells per sample were analyzed using a FACScan flow cytometer (Becton Dickinson) at a rate of 100–200 cells/s. Data were analyzed by CELLQuest software (Becton Dickinson), and the percentage of cells in the phases of the cell cycle was determined as a ratio of the appropriate fluorescent area to the total fluorescent area.

Cell Surface Binding of Annexin V

Cells treated for 72 h with oligonucleotides were harvested after trypsinization, and apoptotic cells were assayed with Annexin V-FITC Apoptosis Detection Kit. Briefly, 5 × 10^5 cells in 100 μl of binding buffer were incubated with 5 μl of Annexin V-FITC for 20 min at room temperature in the dark. PI (final concentration 1 μg/ml) in

100 μl of binding buffer was then added immediately before the flow cytometric analysis (Becton Dickinson). Ten thousand cells per sample were analyzed at a rate of 100–200 cells/s and analyzed as described above. Early apoptotic cells bound to Annexin V-FITC but excluded PI. Cells in late apoptotic stages were labeled with both Annexin V-FITC and PI.

Soft Agar Colony Formation Assay

PC3 cells were transfected with oligonucleotide/Lipofectin complexes as described. After 24 h, 10^3 cells were trypsinized and washed in Ca^{2+}/Mg^{2+}-free PBS (Life Technologies) and plated in 1 ml of RPMI containing 0.3% (w/v) Noble Agar over a 2-ml layer of RPMI with 0.6% agar in six-well plates. The number of colonies was counted using low magnification microscope (4×).

Measurement of Cellular ATP Levels

ATP was extracted with standard lysis buffer as described. The amount of ATP in the experimental samples was normalized per milligram of protein. ATP levels were quantitated by using ATP Determination Kit (Molecular Probes) using the luciferin-luciferase method. Luminescence was measured in a luminometer (Lumat LB9507, EG&G).

Flow Cytometric Analysis of Mitochondrial Membrane Potential and Mitochondrial Mass

Mitochondrial membrane potential was determined by JC-1 fluorescence and analyzed in FL-1 and FL-2 channels of a FACSCalibur (Becton Dickinson) flow cytometer equipped with a single 488-nm argon laser. Briefly, cells were trypsinized and washed in PBS and resuspended in phenol red-free DMEM (Life Technologies) containing JC-1 at 10 μg/ml for 10 min at room temperature in the dark. Stained cells were washed once with PBS before the flow cytometric analysis. For analysis of mitochondrial mass, cells were stained with 10 μM of NAO in phenol red-free DMEM for 10 min at room temperature in the dark and washed once with PBS prior to analysis. A minimum of 10,000 cells/sample was acquired using a log scale for both analysis and data were analyzed using CELLQuest software (Becton Dickinson).

Quantitation of Intracellular Reactive Oxygen Species Levels

H_2DCF-DA and HE were used to determined ROS and superoxide levels (31). Both dyes are nonfluorescent and can freely diffuse into cells. When HE is oxidized to ethidium (E), it intercalates into cellular DNA and fluoresces. Oxidation of H_2DCF-DA yields 2′,7′dichlorofluorescein (DCF), which also fluoresces, and both can be detected by flow cytometry. Cells were harvested by trypsinization, washed with PBS, and stained with 50-μM H_2DCF-DA or 50-μM HE in phenol red-free DMEM for 2 h at 37°C. The mean fluorescence channel numbers of DCF and E were analyzed by flow cytometry in the FL-1 and FL-2 channels, respectively. A minimum of 10,000 cells was acquired for each sample and data were analyzed using CELLQuest software (Becton Dickinson). Histograms were plotted on a logarithmic scale.

Immunohistochemical Staining for 8-Hydroxy-2′-Deoxyguanosine

Immunohistochemical staining for 8-hydroxy-2′-deoxyguanosine (8-OHdG) was carried out as described (32) using monoclonal antibody 1F7. Briefly, cells were seeded and treated with oligonucleotides on glass slides and fixed with 70% ethanol for 10 min. The slides were then treated with RNase (100 μg/ml) in 10-mM Tris-HCl buffer (pH 7.5) at 37°C for 1 h and then with proteinase K (10 μg/ml) at room temperature for 10 min. Cellular DNA was then denatured by treatment with 4-N HCl for 10 min at room temperature and incubated with 50-mM Trizma base (pH 12) for 5 min. Cells were then blocked with 10% normal goat serum in 10-mM Tris (pH 7.5) at 37°C for 45 min. Staining by the primary antibody 1F7 (1:1 dilution in blocking buffer) was carried out at 4°C overnight. After washing with PBS, cells were treated with secondary antimouse IgG (FITC; 1:150 dilution in blocking buffer) at 37°C for 45 min. After washing in PBS (2 × 5 min), cells were stained with PI (1 μg/1 ml) for 45 s at room temperature. The average nuclear fluorescence intensity for a minimum of 50 randomly selected cells (10 cells in each of 5 fields) was determined using a Nikon Eclipse 600 microscope (Nikon Inc., Melville, NY) mounted with a charge-coupled display camera (Hamamatsu C4742-95 (ORCA-100), Bridgewater, NJ) and equipped with image analyzing software (MetaView Imaging System, Universal Imaging Corporation, West Chester, PA).

Results

Antisense Oligonucleotides Complementary to the *bcl*-2 mRNA Down-Regulate *bcl*-2 Protein Expression

A list of oligonucleotides used is found in Table 1. As shown in Fig. 1, G3139 (an 18-mer targeted to the initiation codon region of the *bcl*-2 mRNA) and 2009 (a 20-mer targeted to the *bcl*-2 open reading frame) both down-regulate the expression of *bcl*-2 protein in PC3 cells (3 days after oligonucleotide treatment) to approximately the same extent (99% *versus* 96%; 400-nM concentration in complex with Lipofectin). In addition, G4232, which has the identical sequence to G3139 but contains a C5-methyl group at each cytidine in both CpG motifs, is to within the variability of the experiment just as active as either G3139 or 2009 (94% down-regulation). A G4232 variant, containing a C5-propynyl group at each CpG, behaves identically to G4232 (data not shown). 2006, a 24-mer containing three CpG motifs but is not complementary to any region of the *bcl*-2 mRNA, has some modest, variable anti-*bcl*-2 activity (40% in Fig. 1; range 0–40% in other experiments) 3 days after the transfection. However, 24 h after the transfection, little or no down-regulation of *bcl*-2 protein expression is observed with G3139 or any of the other oligomers, despite the fact that *bcl*-2 mRNA levels are dramatically diminished. Such differences in rates of *bcl*-2 protein *versus* mRNA down-regulation have been previously observed and most likely stem from the heavily membrane-bound character of the *bcl*-2 protein.

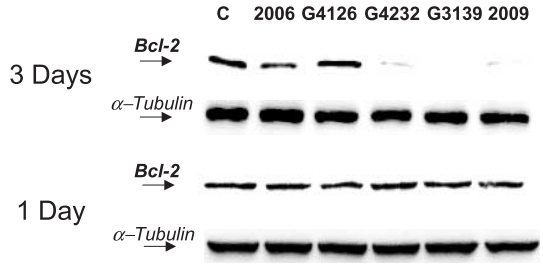

Figure 1. Analysis of *bcl*-2 protein expression in PC3 prostate cancer cells. Cells were treated with complexes of oligonucleotides (400 nM) and Lipofectin (15 μg/ml) for 5 h and harvested after either *1 day* or *3 days*. Protein samples (30–40 μg of protein/lane) were subjected to Western blotting as described in ''Materials and Methods.'' G3139, 2009, and G4232 down-regulated *bcl*-2 protein expression by 99%, 96%, and 94%, respectively, after a 3-day treatment; 2006 caused variable down-regulation of *bcl*-2 protein expression (maximal 40%). *Bcl*-2 protein expression is minimally affected by any oligonucleotide 1 day after treatment.

Anti-*bcl*-2 Oligonucleotides Do Not Cause Significant Apoptosis in PC3 Cells

Despite dramatic decreases in *bcl*-2 protein expression, treatment of PC3 cells on day 1 with anti-*bcl*-2 oligonucleotides (400 nM, 5 h) does not result in significant cellular apoptosis 3 days later. For example, we did not observe cleavage of pro-caspase 3 to caspase 3 on Western blotting (see Fig. 10), nor was caspase activation observed by spectrophotometric measurement of a cleavable chromogenic substrate (data not shown). In addition, by fluorescence-activated cell sorting analysis, we observed only very modest changes in the numbers of cells expressing Annexin V and strongly staining with PI. These data are shown in Fig. 2, in which dot plots of Annexin V and PI staining are presented and where the cells in the right upper quadrant are Annexin V+ and PI+, corresponding to cells that are in late apoptosis/early necrosis. In the control untreated cells and those treated with G4126, only 4.2% and 5.8%, respectively, of cells are undergoing late apoptosis/early necrosis. Cells treated with G3139, G4232, or 2009, all of which dramatically down-regulate *bcl*-2 protein and mRNA expression, cause 10.6%, 7.4%, and 11.1%, respectively, of the cells to undergo late apoptosis/early necrosis. On the other hand, treatment with 2006 (24-mer) actually results in a slightly higher number (14.3%) of cells similarly affected. In striking contrast, when PC3 cells were treated with paclitaxel as a positive control (500 nM, 3 days), 50–60% were late apoptotic/early necrotic.

Mitochondrial Function Is Preserved in G3139-Treated PC3 Cells

As would be expected of cells that are not undergoing apoptosis, mitochondrial function in oligonucleotide-treated cells (400 nM, assay 3 days after treatment) is well preserved. Measurement of ATP production (per mg protein) via luciferase assay demonstrates that it is actually 60% higher in G3139-treated cells than in G4126-treated cells and was similar to what was observed in 2009- or 2006-treated cells (Fig. 3A). Furthermore, determination of the mitochondrial membrane potential $\Delta\Psi_m$ by use of the dye JC-1 (Fig. 3b), which fluoresces green (FL-1 channel) when mitochondria are depolarized and red (FL-2 channel) when polarized, demonstrated little change (34.8% of cells fluorescing in both FL-1 and FL-2 channels for G4126 *versus* 36.9% for G3139). This is in sharp contrast to what was observed when the cells were treated with 1-mM H_2O_2, where a dramatic increase in FL-1 (green) fluorescence was observed, signifying mitochondrial membrane depolarization. However, the number of probable dead cells (no red fluorescence) increased from 5% to 15% when cells were treated with G4126 *versus* G3139. As a control for mitochondrial mass, we evaluated NAO fluorescence via flow cytometry (data not shown). This dye binds to mitochondrial cardiolipin in an energy-independent manner, and the mean fluorescence channel number was found to be similar in control and oligonucleotide-treated cells, suggesting that mitochondrial mass in these cells remains relatively constant.

Despite Preservation of Mitochondrial Potential, G3139 Still Dramatically Influences the Rate of Proliferation of PC3 Cells

For example, both G3139 and 2006 (but not G4126) dramatically reduced the ability of PC3 cells to clone in soft

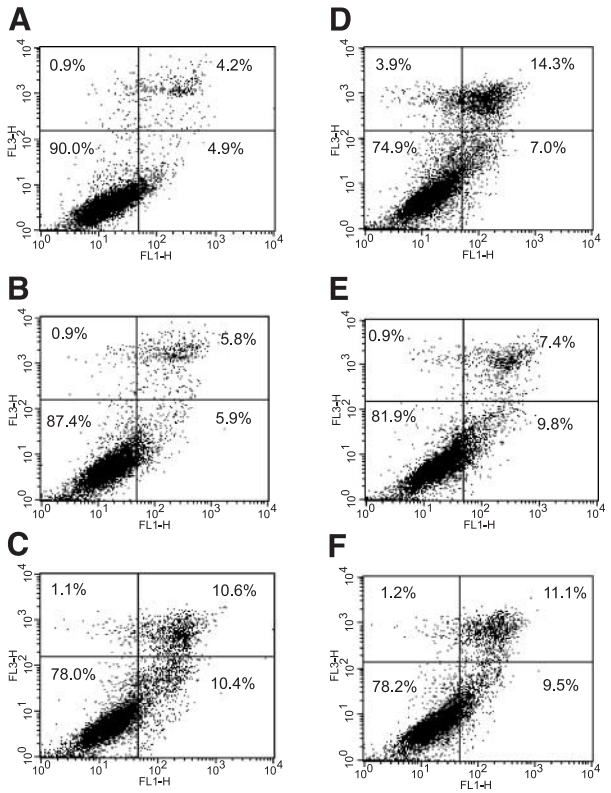

Figure 2. Flow cytometric analysis of oligonucleotide-treated PC3 cells analyzed after fluoresceinated anti-Annexin V monoclonal antibody binding (*X* axis) and PI uptake (*Y* axis). *Dots in upper right quadrant,* late apoptosis/early necrosis; *dots in lower right quadrant,* early apoptosis; *dots in upper left quadrant,* necrosis. Assays were performed 3 days after a 5-h transfection of the cells with 400-nM oligonucleotides complexed to Lipofectin (15 μg/ml). Untreated cells (**A**), G4126 (**B**), G3139 (**C**), 2006 (**D**), G4232 (**E**), and 2009 (**F**). None of the oligonucleotides caused significant apoptosis in the PC3 cells.

agar (Fig. 4A). In addition, the rate of cell proliferation in complete media, where the number of living cells was assessed by trypan blue exclusion, was drastically diminished for up to 6 days by G3139 and 2006 but not by G4126 (Fig. 4B). In addition, G4232, which down-regulates *bcl*-2 expression to the same extent as G3139 but has both CpG cytidines methylated, affected the rate of cell proliferation approximately only to the same modest extent as G4126. The relative lack of growth suppression *versus* G3139 is not specific only to the C5 methylation found in G4232; C5 propynylation of both CpG motifs also produces lack of suppression of cell proliferation *versus* what was observed with G3139. However, C5 methylation of cytosines not present in the CpG motif (84825) did not produce inhibition of cell growth. Moreover, both CpG cytosines were required to produce maximum inhibition of cell growth. In experiments in which only one CpG cytosine was methylated (84822 and 84823), the rate of cell growth was independent of the cytosine methylated and was intermediate between those observed with G4126 and G3139 (Fig. 4c). However, the effects of the CpG motifs on PC3 cell proliferation are unlike those produced when immunocompetent cells are treated with CpG-containing phosphorothioate oligodeoxynucleotides. Naked G3139 (*i.e.*, uncomplexed with Lipofectin, up to 10 μM) did not inhibit the rate of cell proliferation, demonstrating that adequate intracellular (and perhaps intranuclear) concentrations of G3139 are required.

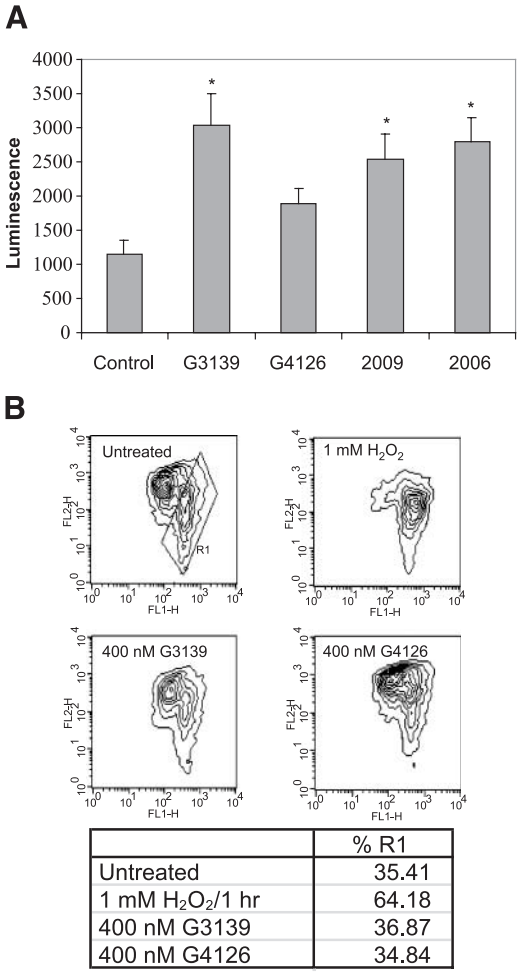

	% R1
Untreated	35.41
1 mM H_2O_2/1 hr	64.18
400 nM G3139	36.87
400 nM G4126	34.84

Figure 3. **A,** ATP production by PC3 prostate cancer cells after treatment with oligonucleotide/Lipofectin complexes. Cells were treated and harvested as described in ''Materials and Methods.'' Cellular ATP samples were normalized to protein content as determined by the Bradford assay. Experiments were done in triplicate. *Columns,* mean; *bars,* SD. *, $P < 0.05$, by Student's *t* test assuming unequal variances. (Control not included in analysis: All comparisons made to G4126 to eliminate nonspecific oligonucleotide treatment.) **B,** flow cytometric analysis of the mitochondrial membrane potential of PC3 prostate cancer cells as assessed by JC-1 staining. *%R1* are cells with depolarized mitochondria, as measured by the reversible shift in JC-1 fluorescence emission from *red* (FL-2 channel) to *green* (FL-1 channel). A positive control was performed using 1-mM H_2O_2 treatment for 1 h. The results from both the ATP production study and the evaluation of mitochondrial membrane potential indicate the integrity of mitochondrial respiration after treatment with oligomer/Lipofectin complexes.

Truncation Variations of G3139 Down-Regulate *bcl*-2 Protein Expression

Additional data also may relate to the critical role of the CpG motifs and suggest that the down-regulation of *bcl*-2 protein expression may occur not only via an antisense mechanism but also by other mechanisms. The ability of G3139-related anti-*bcl*-2 oligonucleotides to down-regulate the expression of *bcl*-2 protein is dramatically dependent on the length of the oligomer (Table 2). We created a series of truncation mutations in which single bases were progressively deleted from either the 5′ or the 3′ terminal end of G3139. Only one to two bases could be removed from the 3′ terminal end without significant loss of anti-*bcl*-2 activity. In contrast, about seven to eight bases could be removed from the 5′ terminal end without similar loss.

Inhibition of Cell Proliferation Is Associated with the Generation of Reactive Oxygen Species

Treatment of PC3 cells with G3139 causes a dramatic increase in the intracellular production of ROS, as assessed by oxidation of HE → E, which subsequently intercalates with fluorescence detectable by flow cytometry. We also employed an alternative method, not dependent on intercalation of DNA, involving the oxidation of cell-permeable H_2DCF-DA to fluorescent DCF. G3139 causes an increase in the production of ROS as measured by E fluorescence by as much as 500% *versus* untreated cells (range 200–500%; Fig. 5A) and by DCF fluorescence (as much as 250%; Fig. 5B). Maximum generation of ROS was observed ~72 h after oligonucleotide treatment, but ROS generation could still easily be observed for 5 days after the initial treatment. Although maximum generation of ROS was observed at the same time as maximum down-regulation of *bcl*-2 protein activity, the latter does not cause the former. This is demonstrated by the fact that neither G4232 (or the C5-propynylated variant) nor 2009 (all 400 nM), both of which maximally down-regulate the expression of *bcl*-2 protein after 3 days, cause a significantly greater increase in the production of ROS (*versus* control untreated cells) than does G4126 (400 nM; Fig. 5C).

Furthermore, the production of ROS (HE → E) is highly concentration dependent (maximum at 400 nM, absent at 100 nM) and is closely linked to the rate of cellular proliferation; cells virtually stop growing at 400 nM, but cell proliferation is still slightly diminished at 100 nM. Nevertheless, the generation of ROS is not linked to the down-regulation of *bcl*-2 protein expression, the extent of which was similar at 100 and 400 nM (Fig. 6a). However, *bcl*-2 mRNA expression (relative to G4126), by Northern analysis, was down-regulated only at 400 nM but not at 200 or 100 nM, also indicating the presence of an additional non-antisense mechanism of action (Fig. 6B).

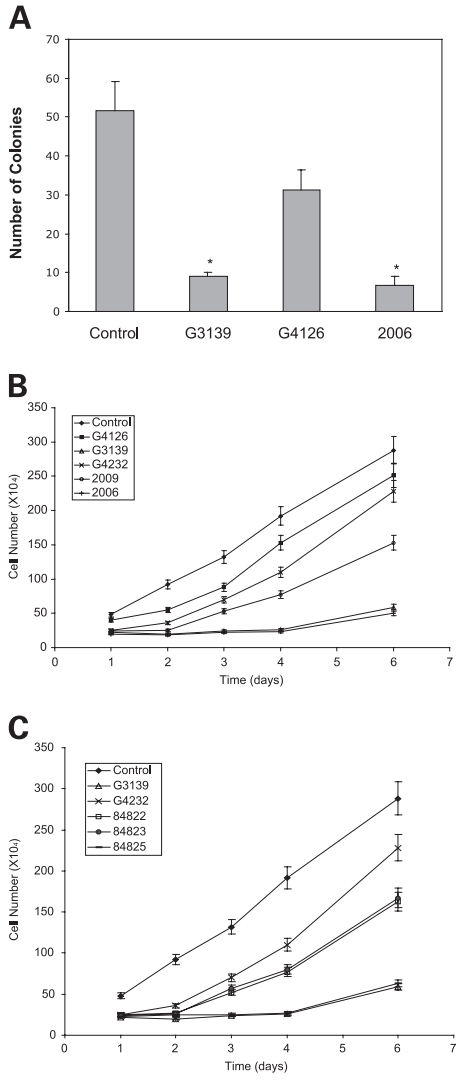

Figure 4. **A,** rate of proliferation of PC3 prostate cancer cells is greatly reduced by treatment with oligomers containing CpG motifs, as assessed by (**A**) soft agar colony formation assay and (**B** and **C**) trypan blue exclusion. G3139 and 2006 caused a dramatic inhibition in cloning efficiency and cellular proliferation after 6 days (**A** and **B**). **B,** G4126 and G4232 only slightly affected the proliferation rate, whereas the effect of 2009, a two-base longer oligomer, is intermediate. **C,** 84825 (C5 methylation outside the CpGs) inhibited cell proliferation to the same extent as G3139. However, oligonucleotides with only a single C5-methylated CpG (84822 and 84823) considerably lessen the inhibitory effect on cell proliferation. *Lines,* average; *bars,* SD ($n = 3$). *, $P < 0.05$, by Student's *t* test assuming unequal variances. (Control not included in analysis: All comparisons made to G4126 to eliminate nonspecific oligonucleotide treatment.)

However, it should be noted that the production of ROS is very closely linked to cellular confluency (33). After 3 days in culture, control untreated and G4126- and 2009-treated cells are confluent, unlike G3139- and 2006-treated cells. Thus, although the rate of proliferation of these treated cells is minimal, their production of ROS is in fact more appropriate for cells that are rapidly proliferating.

Mutant G3139-Related Oligomers Generate Reactive Oxygen Species and Down-Regulate *bcl*-2 Protein Expression

We then created a series of mutant G3139-related oligomers (Table 1) designed to further establish the role of the CpG motifs in the generation of ROS (which appears to be intimately related to inhibition of cell proliferation). As shown, the average mean fluorescence channel number (E fluorescence) of cells treated with G3139, G4263 (two-base mismatch), and G4264 (four-base mismatch), all of which preserve the bis-CpG motif, was ~218. In contrast, in G4126-treated cells (two-base mismatch, elimination of both CpG motifs), the mean channel number was only ~115 (Fig. 7B). Interestingly, both G4263 and G4264 down-regulated *bcl*-2 protein expression, but to a somewhat lesser extent than G3139 (Fig. 7A). Strikingly, increasing the number of mismatches to 6, 8, and even 12, provided the CpG motifs were preserved, still allowed for the down-regulation of *bcl*-2 protein expression (Fig. 8A) and for the generation of ROS (Fig. 8B). However, the 12-base mismatched oligomer was not as efficient as the 8-base mismatched species.

Treatment of PC3 Cells with G3139 Results in Oxidation of Nuclear Guanosine to 8-Hydroxy-2′-Deoxyguanosine

To determine if the production of ROS was linked to the oxidation of nuclear DNA, cells treated with G3139 and related oligomers were stained for 8-OHdG using the 1F7 monoclonal antibody, and cellular fluorescence was quantitated. As positive and negative controls, peripheral blood lymphocytes were treated with H_2O_2 (Fig. 9, A and B). The results demonstrate that nuclear staining with 1F7 is significantly greater for G3139 (Fig. 9D) than for control untreated cells (Fig. 9C) and also than for any of the other oligomers tested (G4126, 2006, or 2009; Fig. 9, e–g, respectively), with the possible exception of G4232 (Fig. 9h). The quantitation of these results is presented in Fig. 9i.

G3139 Induces a G_1-S Entry Block and an Intra-S-Phase Block

As demonstrated, G3139 does not induce a significant amount of apoptosis or necrosis but does dramatically inhibit the rate of cellular proliferation. We thus performed double labeling studies with BrdUrd and PI to examine the relative proportion of cells in each phase of the cell cycle and the rate of oligonucleotide-treated cell progression through the cell cycle. (It should be noted that usual cell

Table 2. Down-regulation of *bcl*-2 protein expression in G3139 truncation mutants

Oligonucleotide	% Inhibition of *bcl*-2 protein[a]
3′ Truncation mutations	
5′-TCT CCC AGC GTG OGC CAT-3′	84
TCT CCC AGC GTG OGC CA	84
TCT CCC AGC GTG OGC C	37
5′ Truncation mutations	
5′-TCT CCC AGC GTG OGC CAT-3′	90
CT CCC AGC GTG OGC CAT	85
T CCC AGC GTG OGC CAT	84
CCC AGC GTG OGC CAT	85
C AGC GTG OGC CAT	85
GC GTG OGC CAT	68
GTG OGC CAT	16

[a]As determined by Western blotting and laser scanning densitometry as described in text.

cycle synchronization techniques fail due to toxicity when the cells are treated with phosphorothioate oligonucleotides in combination with synchronizing agents.) The dot plot data in Fig. 10 show cells 1 day after a 5-h treatment with the oligomers, as described in ''Materials and Methods.'' These cells were harvested 0, 4, 8, and 20 h after a 2-h pulse with BrdUrd. At this time, as demonstrated previously, *bcl*-2 protein expression is only minimally down-regulated (see Fig. 1). However, the number of cells that were in S phase at 24 h (BrdUrd+) declined (Table 3) from 43% (control) to 31% (G4126 treated) to 19% (G3139 treated), signifying a block of entry of cells from G_1 into S. Furthermore, the proportion of cells at 24 h in S phase that were BrdUrd− increased from ~3.5% (control) to 4% (G4126 treated) to 11% (G3139 treated), denoting a block in the progression of cells through S phase. However, the difference in the number of S-phase cells that did not incorporate BrdUrd diminished relative to control untreated and G4126-treated cells as a function of time after the pulse. However, if cells were pulsed with BrdUrd 3 days after they were transfected with oligonucleotide (data not shown), the results were virtually identical to what we observed in Fig. 10 and Table 3.

We then examined various S-phase genes by Western blotting to see if their expression was affected after treatment by G3139 and related oligonucleotides. These data are shown in Fig. 11; the expression of c-*myb* protein was decreased in G3139-treated *versus* G4126-treated cells by ~80%. PARP, also an S-phase gene, is decreased by almost 90%, but PARP cleavage products, which would have signified apoptosis, were absent, as were pro-caspase 3 cleavage products. However, the expression of neither cyclin D1, cdk4, nor cdk2 proteins was changed at 3 days, demonstrating that the expression of only certain S-phase genes was down-regulated by treatment with G3139.

Discussion

G3139, as measured by lack of Annexin V binding and PI uptake (Fig. 2), preservation of mitochondrial $\Delta\Psi_m$ and production of ATP (Fig. 3), and lack of evidence of either PARP and pro-caspase 3 cleavage (Fig. 11), appears to cause little in the way of cellular apoptosis. In addition, as

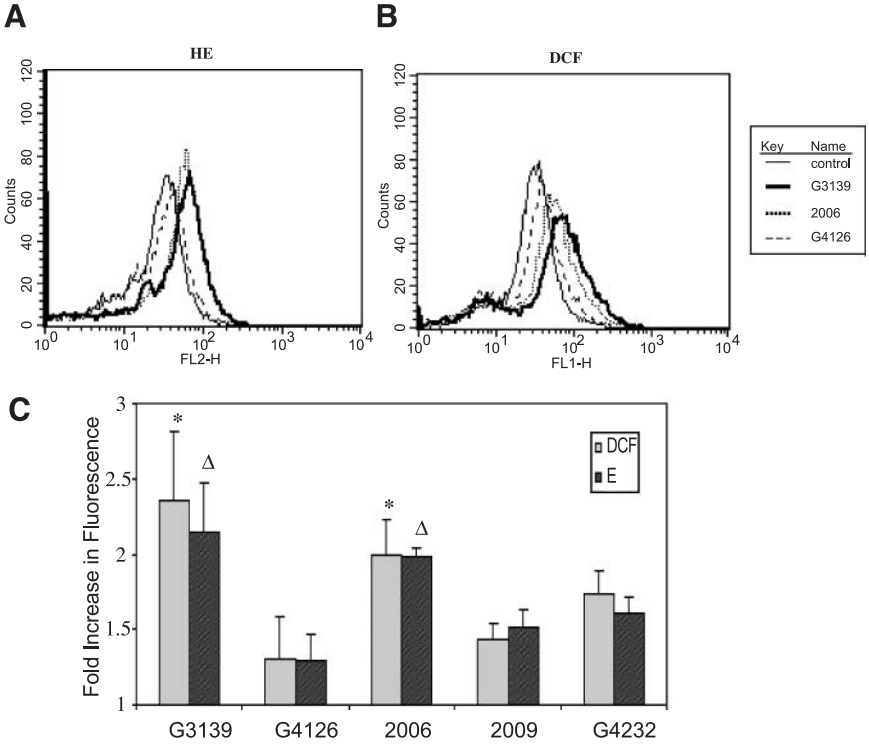

Figure 5. Flow cytometric analysis of ROS production in oligonucleotide-treated PC3 prostate cancer cells as demonstrated by the oxidation of H_2DCF → DCF and HE → E. Cells were treated with oligomer (400 nM)/Lipofectin (15 μg/ml) complexes for 3 days as described. **A** and **B**, representative histograms of the mean fluorescence channels of DCF and E fluorescence from one of three experiments. G3139 and 2006 caused a significant shift (more than 2-fold increase) in fluorescence of both markers of ROS production. **C,** a summary of ROS production by different oligomers. Fold increase in mean fluorescence channel was normalized against untreated cells. *Columns,* average; *bars,* SD (n = 3). * and Δ, $P < 0.05$, by Student's t test assuming unequal variances. (Control not included in analysis: All comparisons made to G4126 to eliminate nonspecific oligonucleotide treatment.)

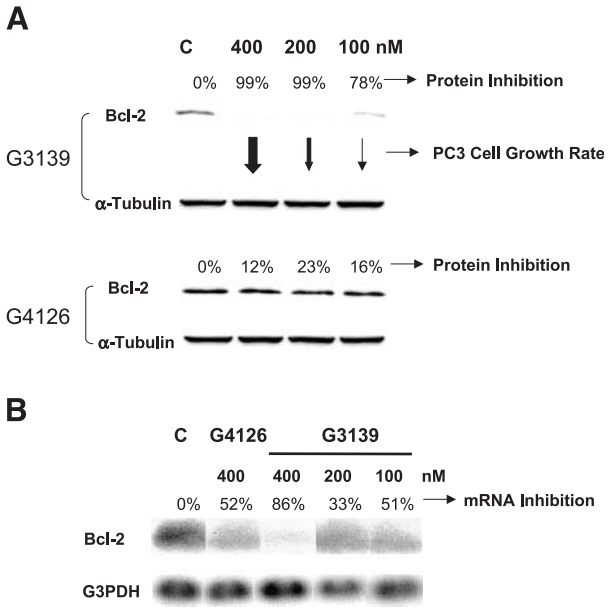

Figure 6. **A,** G3139 down-regulates *bcl*-2 protein expression in PC3 prostate cancer cells by a similar extent at 400, 200, and 100 nM (99%, 99%, and 78%, respectively; representative of three experiments) as demonstrated by Western blotting (performed as described in the text). Cells were transfected with oligonucleotide/Lipofectin complexes for 5 h and then incubated in complete media without these complexes for an additional 68 h. The rate of cell growth, as determined by trypan blue exclusion, was significantly inhibited at 400 nM, although minimally decreased at 200 and 100 nM. G4126 did not affect *bcl*-2 protein expression and only minimally affected the growth rate of PC3 cells at these concentrations. **B,** Northern analysis (composite picture from the same gel) of *bcl*-2 mRNA expression in G3139- and G4126-treated PC3 cells as a function of oligonucleotide concentration. Cells were treated as in **A** and harvested after 19 h. The nonspecific effect of G4126 (400 nM) on *bcl*-2 mRNA (52%) expression can be seen.

evaluated by BrdUrd/PI uptake, G3139 (compared with G4126) causes a partial block in S-phase entry and in progression through S phase (Table 3; Fig. 10). This block in S phase is reflected in the diminution of expression of certain S-phase-specific genes (*e.g.*, c-*myb* and PARP; Fig. 11; 34, 35) and probably leads to the dramatic decrease in the rate of cell proliferation as shown in Fig. 4, b and c.

However, G3139, as opposed to G4232 and 2009 (which at 20 bases is slightly longer than G3139), appears to be strongly cytostatic, with almost no cell growth occurring until 5–6 days after oligonucleotide/Lipofectin transfection. Because each of these oligomers down-regulates *bcl*-2 protein expression to essentially the same extent after 3 days but do not produce the same phenotype, then it seems likely that other mechanisms rather than just *bcl*-2 down-regulation are at least in part responsible for the production of the growth-inhibited phenotype.

However, a caveat should be raised in that these results should not be extrapolated to other cell types or to what occurs clinically. Nevertheless, we have seen parallel results in T24 bladder carcinoma cells (J. Lai, personal observations) and speculate that other cell lines may behave similarly. It must also be pointed out that other classes of phosphorothioate oligodeoxynucleotides (*e.g.*, 2′-*O*-methyloligoribonucleotide/oligodeoxyribonucleotide gap-mers) may be more specific than the all-oligodeoxyribonucleotide phosphorothioates. Treatment of cells with a G3139 gap-mer may potentially vitiate some of the effects we have observed.

Our findings suggest that inhibition of cellular proliferation may occur as a result of a specific oligonucleotide sequence motif, which we call the ''bis-CpG'' motif to distinguish it from the ''classical'' single CpG motif that activates immunocompetent cells (36). Maximum inhibition of cell proliferation by G3139 appears to require both CpG motifs, as C5 methylation of only a single CpG (*e.g.*, in 84822 and 84823) does not fully suppress growth. 2009, although longer than G3139, does not contain any CpG motifs and does not suppress cell growth to nearly the same extent as G3139. G4126, in which both CpG motifs have been mutated, is only minimally growth suppressive.

Thus, it may not be necessary to invoke a RNase H-dependent antisense mechanism of action to explain the

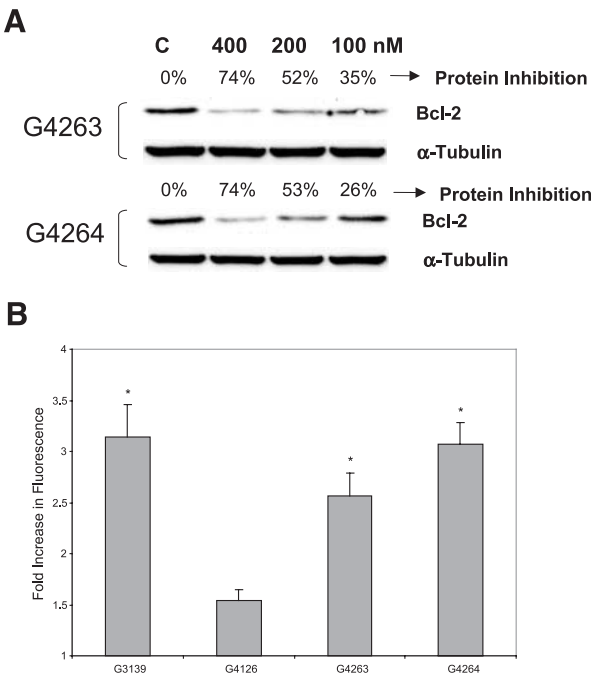

Figure 7. **A,** G4263 and G4264 (each 400 nM), which contain two- and four-base mismatches but have preserved the CpG motifs, each down-regulated *bcl*-2 protein expression in PC3 prostate cancer cells by 74% as determined by Western blotting analysis and laser scanning densitometry (representative of three experiments). The dose-dependent inhibition of *bcl*-2 protein expression is also demonstrated. Cells were treated with complexes for 5 h as described in ''Materials and Methods'' and harvested after 3 days. **B,** production of ROS by PC3 cells after a 3-day treatment of oligomer (400 nM)/Lipofectin complexes as assessed flow cytometrically by HE → E oxidation. G4263 and G4264 caused a relatively similar increase (*versus* G4126) in the generation of ROS as compared with G3139. The fold increase in fluorescence was compared with the untreated cells. *Columns,* average; *bars,* SD (n = 3). *, $P < 0.05$, by Student's t test assuming unequal variances. (Control not included in analysis: All comparisons made to G4126 to eliminate nonspecific oligonucleotide treatment.)

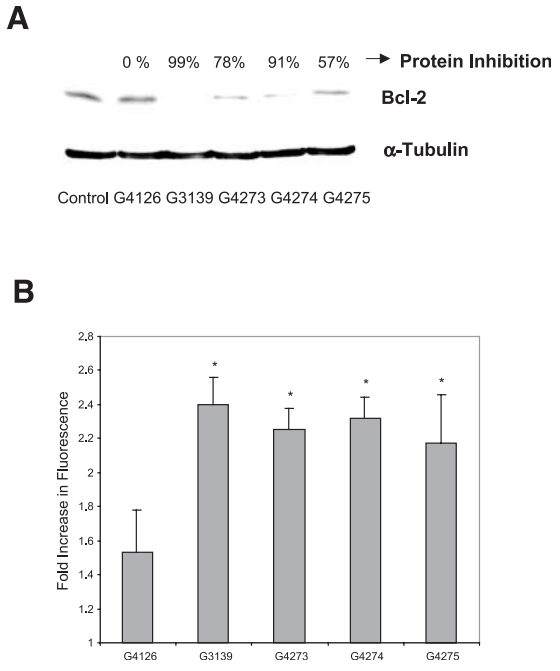

Figure 8. **A,** G4273, G4274, and G4275, which contain 6, 8, and 12 mismatches but have preserved the CpG motifs, down-regulated *bcl*-2 protein expression by 78%, 91%, and 57%, respectively, as determined by Western blotting analysis and laser scanning densitometry. Cells were treated with oligonucleotide (400 nM)/Lipofectin (15 μg/ml) complexes as described previously. **B,** production of ROS by PC3 cells 3 days after a 5-h treatment of oligomer (400 nM)/Lipofectin complexes, as assessed flow cytometrically by HE → E oxidation. G4273, G4274, and G4275 caused an extensive increase in ROS level, similar to G3139. *Columns,* average; *bars,* SD (n = 3). *, $P < 0.05$, by Student's t test assuming unequal variances. (Control not included in analysis: All comparisons made to G4126 to eliminate nonspecific oligonucleotide treatment.)

down-regulation of the expression of *bcl*-2 protein by G3139 and related oligonucleotides. Down-regulation of *bcl*-2 protein expression was observed with mismatched variants of G3139, including G4263 (two-base mismatch outside the two CpG motifs) and G4264 (four-base mismatch outside the two CpG motifs), but not with G4126 (two-base mismatch in which both CpG motifs are destroyed). In addition, G4273, G4274, and G4275 (containing 6-, 8-, and 12-base mismatches *versus* G3139, respectively, but preserving the ''bis-CpG'' motif) also down-regulate *bcl*-2 protein expression and, similar to G3139, increase cellular ROS production as measured by HE → E oxidation. None of these oligonucleotides can possibly work via a RNase H-dependent antisense mechanism.

It should also be noted, however, that G4275 (12-base mismatches) is significantly less active than the others; we speculate that that this may be due to the fact that additional sequence motifs in the molecule may potentiate the effect of the ''bis-CpG'' motif. Some evidence for this speculation may be adduced from the data in Table 2, in which both 3′ and 5′ truncation mutations of G3139 were evaluated for their ability to down-regulate the expression of *bcl*-2 protein. G3139 is significantly less tolerant to 3′ truncation than 5′ truncation with respect to retention of anti-*bcl*-2 activity. This is possibly because these hypothesized additional sequence motifs are closer to the 3′ molecular terminal end.

In addition, although other explanations are possible, it seems unlikely that the truncation mutations cause *bcl*-2 down-regulation via an antisense mechanism. Because a 16-mer product of 3′ truncation cannot down-regulate *bcl*-2 protein expression, the 11- and 13-mer phosphorothioate oligonucleotide products of 5′ truncation would certainly

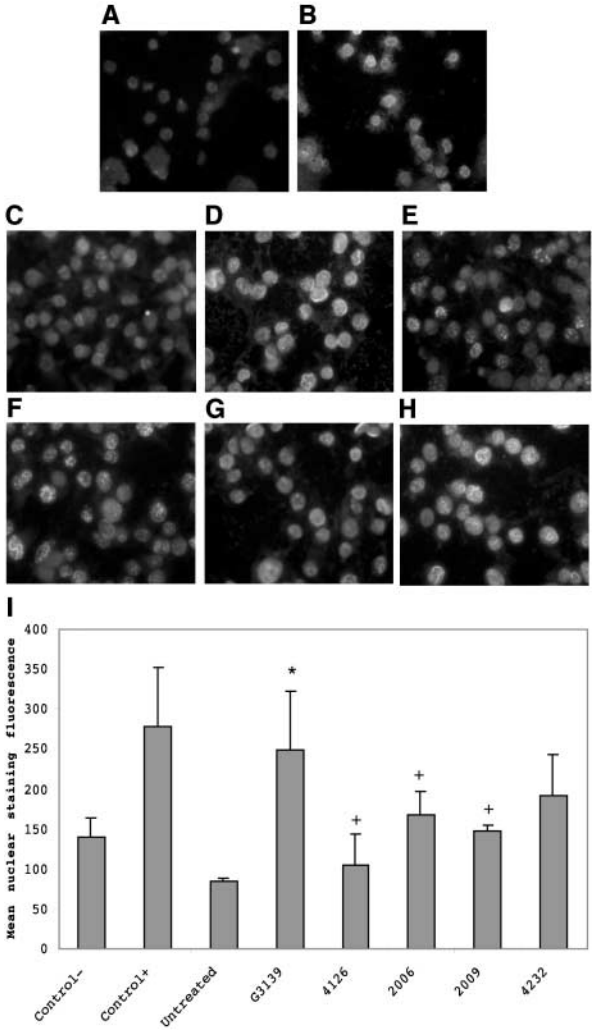

Figure 9. Immunohistochemical detection of 8-OHdG by use of the 1F7 monoclonal antibody in oligomer-treated PC3 prostate cancer cells. **A,** control untreated peripheral blood lymphocytes. **B,** peripheral blood lymphocytes treated with 4.4-M H_2O_2 for 15 min. Photomicrographs of untreated PC3 prostate cancer cells (**C**) and cells treated with G3139 (**D**), G4126 (**E**), 2006 (**F**), 2009 (**G**), and G4232 (**H**). Before the immunohistochemical analysis, cells were treated with oligonucleotide (400 nM)/Lipofectin (15 μg/ml) complexes as described. **I,** mean nuclear staining (average fluorescence) by 1F7 for 8-OHdG demonstrated a significant difference between untreated and G3139-treated cells. *Columns,* mean; *bars,* SD (n = 5). *, P = 0.004, difference between G3139 and untreated cells. +, P = 0.004, 0.04, and 0.04, differences between G3139 and G4126, 2006, and 2009, respectively, as analyzed by Student's t test assuming unequal variances. (P = 0.21 for G4232.)

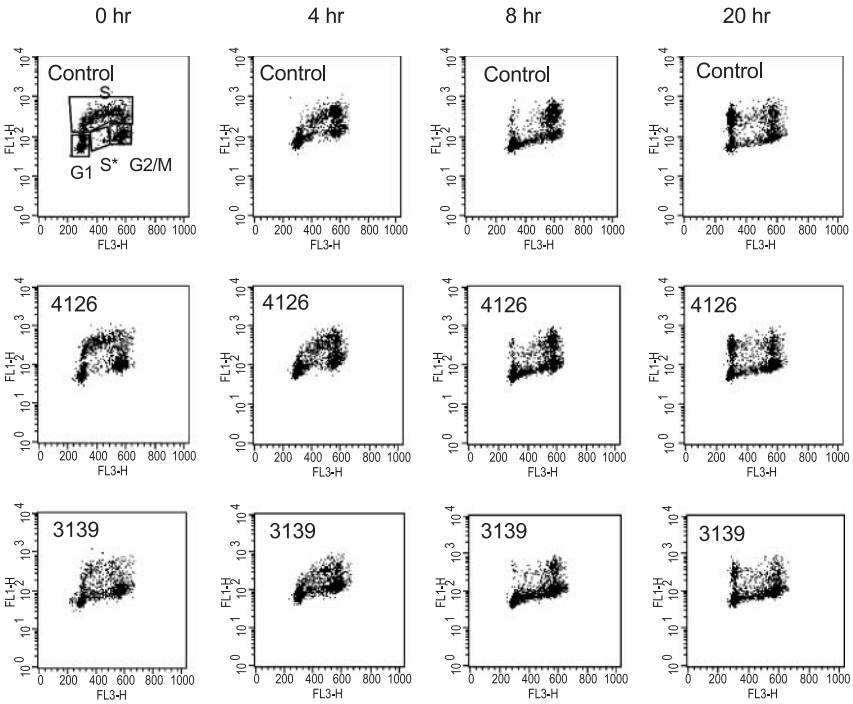

Figure 10. Flow cytometric analysis of BrdUrd incorporation (*Y* axis; FL-1 channel) and DNA content as determined by PI staining (*X* axis; FL-3 channel) in oligomer-treated PC3 cells. Cells were either untreated or treated for 5 h with G4126 (400 nM)/Lipofectin (15 μg/ml) or G3139 (400 nM)/Lipofectin (15 μg/ml). Nineteen hours later, as described in ''Materials and Methods,'' cells were pulsed with 10-μM BrdUrd for 2 h. Cells were harvested and analyzed 0, 4, 8, and 20 h after the BrdUrd pulse. (Region gates for the quantitative analysis are indicated.) Integrated data are presented in Table 3.

not be long enough to support an antisense mechanism of action. This, in turn, indicates that the down-regulation of *bcl*-2 protein expression by this truncated oligomer probably occurs via another yet unknown but non-antisense mechanism.

However, some nonspecific effects on cellular proliferation were observed with essentially all the phosphorothioate oligonucleotides used in this study. To block cell proliferation, the ''bis-CpG'' motif must act in the context of an oligonucleotide of the appropriate length. Thus, while 2006 (24-mer) suppresses cell growth to the same extent as G3139 and contains ''optimized'' CpG motifs, 2006-1, which is an 18-mer also containing ''optimized'' CpG motifs, does not recapitulate the G3139 phenotype.

Table 3. Analysis of cell cycle phases in oligonucleotide treated cells

Oligomers	G_1 (%)	S (%)	G_2-M (%)	S* (non-BrdUrd incorporating) (%)
Control, 0 h	32.40	42.70	17.50	3.50
G4126, 0 h	36.80	31.10	23.10	4.10
G3139, 0 h	40.30	18.80	25.20	11.00
Control, 4 h	37.90	37.20	15.50	5.80
G4126, 4 h	42.20	29.10	16.00	6.40
G3139, 4 h	41.60	22.20	21.10	10.30
Control, 8 h	26.90	38.90	13.50	17.30
G4126, 8 h	29.90	32.40	15.50	18.40
G3139, 8 h	33.40	22.10	20.10	19.60
Control, 20 h	15.50	48.40	26.20	7.20
G4126, 20 h	20.60	39.50	27.50	9.10
G3139, 20 h	27.70	27.00	29.50	12.30

Note: The percentage of BrdUrd-incorporated cells in S phase greatly diminished in G3139-treated cells, whereas the percentage of S* (non-BrdUrd-incorporating cells) is significantly higher compared with the untreated and G4126-treated cells, demonstrating a block of entry of G3139-treated cells from G_1 into S phase and in the progression of cells through S phase. Note that the difference in the number of S-phase (G3139-treated) cells that did not incorporate BrdUrd diminished relative to untreated and G4126-treated cells as a function of time after the pulse.

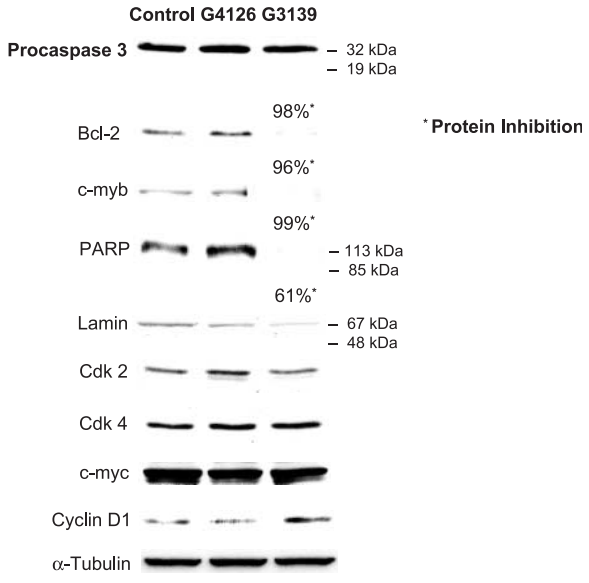

Figure 11. Representative Western blot analyses of S-phase and other proteins from PC3 cell lysates obtained 3 days after oligomer (400 nM)/Lipofectin (15 μg/ml) treatment. Approximately 30–40 μg of protein samples were loaded in each lane. No change in the level of expression of pro-caspase 3 protein or in its cleavage to caspase 3 was observed after treatment with oligonucleotides. Compared with G4126, G3139 dramatically down-regulated the expression of several S-phase genes, including c-*myb* and PARP. However, no PARP cleavage products were observed. Levels of cdk2, cdk4, c-*myc*, α-tubulin, and cyclin D1 expression also remained essentially unaltered after 3 days.

It is important to note that the G3139 phenotype (*i.e.*, inhibition of cellular proliferation) can be significantly recapitulated by increasing the concentration of the ''inactive'' oligomer G4126 to 800–1000 nM. This suggests that two ''nonspecific'' mechanisms contribute to the antiproliferative effect of phosphorothioate oligonucleotides. One of these mechanisms is highly length (and concentration) dependent and is facilitated by the other that appears to be dependent on the presence of the ''bis-CpG'' motif. The higher the oligomer concentration and length, the less important is the latter bis-CpG mechanism.

There appears to be a correlation between the inhibition of cell proliferation and the generation of ROS. As has been demonstrated (33), when cells become confluent, and thus growth arrested, the production of ROS dramatically diminishes. However, cells treated with G3139, which are *de facto* growth arrested, produce similar amounts of ROS, as do cells that are in log-phase growth. Because the preponderance of ROS is derived from mitochondrial respiration, this observation correlates with the fact that the mitochondrial $\Delta\Psi_m$ remains intact and ATP production is undiminished. However, in G3139-treated cells, the production of cellular ATP and ROS has effectively been decoupled from the process of cellular proliferation. One consequence of increased ROS production appears to be oxidation of nuclear guanosine to 8-OHdG, as measured by immunochemical staining by 1F7. The effects of G3139 treatment on guanosine oxidation, at least in some experiments, can be almost as marked as what is observed after short-term treatment with 1-mM H_2O_2. Furthermore, 2009 does not produce oxidation of nuclear guanosine although it down-regulates *bcl*-2 protein expression to the same extent as G3139. However, 2009 causes little in the way of ROS production. On the other hand, 2006, which causes an increase in ROS production but not to the extent of G3139, causes a small increase in 8-OHdG production (*versus* control). Curiously, however, G4232 only partially blocks 8-OHdG production, but this may be more a reflection of the intrinsic variability of the assay than of mechanistic relevance. Nevertheless, when taken together, these results suggest that the combination of *bcl*-2 down-regulation and production of ROS leads to oxidation of nuclear DNA. These results are concordant with those of Hockenberry *et al.* (10) and suggest that *bcl*-2 protein, similar to its protective effect over mitochondria, may also be protective of the integrity of nuclear DNA with respect to oxidation.

Acknowledgments

We thank Amanda Gillum and Robert Klem of Genta for supplying many of the oligonucleotides used in this paper.

References

1. Reed, J. C. Bcl-2 and the regulation of programmed cell death. J. Cell Biol., *124:* 1 – 6, 1994.

2. Reed, J. C. Bcl-2: prevention of apoptosis as a mechanism of drug resistance. Hematol. Oncol. Clin. N. Am., *9:* 451 – 473, 1995.

3. Reed, J. C., Jurgensmeier, J. M., and Matsuyama, S. Bcl-2 family proteins and mitochondria. Biochim. Biophys. Acta, *1366:* 127 – 137, 1998.

4. Hockenberry, D., Nunez, G., Milliman, C., Schreiber, R., and Krosmeyer, S. Bcl-2 is an inner mitochondrial membrane protein that blocks programmed cell death. Nature, *348:* 334, 1990.

5. Krajewski, S., Tanaka, S., and Takayama, S. Investigation of the subcellular distribution of the *bcl*-2 oncoprotein: residence in the nuclear envelope, endoplasmic reticulum and outer mitochondrial membranes. Cancer Res., *53:* 4701, 1993.

6. De Jong, D., Prins, F., and Mason, D. Subcellular localization of the *bcl*-2 protein in malignant and normal lymphoid cells. Cancer Res., *54:* 256 – 260, 1994.

7. Zhu, W., Cowie, A., and Wasfy, G. Bcl-2 mutants with restricted subcellular location reveal spatially distinct pathways for apoptosis in different cell types. EMBO J., *15:* 4130, 1996.

8. Schlesinger, P., Gross, A., and Yin, X. Comparison of the ion channel characteristics of proapoptotic BAX and antiapoptotic BCL-2. Proc. Natl. Acad. Sci. USA, *94:* 11357, 1997.

9. Vander Heiden, M., Chandel, N., Schumacker, P., and Thompson, C. Bcl-xL prevents cell death following growth factor withdrawal by facilitating mitochondrial ATP/ADP exchange. Mol. Cell, *3:* 159 – 167, 1999.

10. Hockenberry, D., Oltvai, Z., Yin, X., Milliman, C., and Krosmeyer, S. Bcl-2 functions in an antioxidant pathway to prevent apoptosis. Cell, *75:* 241 – 251, 1993.

11. Zhong, L., Sarafian, T., Kane, D., Charles, A., Mah, S., Edwards, R., and Bredesen, D. Bcl-2 inhibits death of central neural cells induced by multiple agents. Proc. Natl. Acad. Sci. USA, *90:* 4533 – 4537, 1993.

12. Kane, D., Sarafian, T., Anton, R., Hahn, H., Gralla, E., Valentine, J., Ord, T., and Bredesen, D. Bcl-2 inhibition of neural death: decreased generation of reactive oxygen species. Science, *262:* 1274 – 1277, 1993.

13. Miyashita, T. and Reed, R. C. Bcl-2 oncoprotein blocks chemotherapy-induced apoptosis in a human leukemia cell line. Blood, *81:* 151 – 157, 1993.

14. Walton, M. I., Whysong, D., O'Connor, P. M., Hockenberry, D., Korsmeyer S. J., and Kohn, K. W. Constitutive expression of human Bcl-2 modulates nitrogen mustard and campothecin induced apoptosis. Cancer Res., *53:* 1853 – 1861, 1993.

15. Kamesaki, S., Kamesaki, H., Jorgensen, T. J., Tanizawa, A., Pommier, Y., and Cossman, J. Bcl-2 protein inhibits etoposide-induced apoptosis through its effects on events subsequent to topoisomerase II-induced DNA strand breaks and their repair. Cancer Res., *53:* 4251 – 4256, 1993.

16. Tang, C., Willingham, M. C., Reed, J. C., Miyashita, T., Ray, S., Ponnathpur, V., Huang, Y., Mahoney, M. E., Bullock, G., and Bhalla, K. High levels of p26BCL-2 oncoprotein retard taxol-induced apoptosis in human pre-B leukemia cells. Leukemia, *8:* 1960 – 1969, 1994.

17. Teixeira, C., Reed, J. C., and Pratt, M. A. Estrogen promotes chemotherapeutic drug resistance by a mechanism involving Bcl-2 proto-oncogene expression in human breast cancer cells. Cancer Res., *55:* 3902 – 3907, 1995.

18. Pratt, M. A., Krajewski, S., Menard, M., Krajewski, M., Macleod, H., and Reed, J. C. Estrogen withdrawal-induced human breast cancer tumor regression in nude mice is prevented by Bcl-2. FEBS Lett., *440:* 403 – 408, 1998.

19. Dorai, T., Perlman, H., Walsh, K., Shabsigh, A., Golubof, E. T., Olsson, C. A., and Buttyan, R. A recombinant defective adenoviral agent expressing anti-*bcl*-2 ribozyme promotes apoptosis of *bcl*-2-expressing human prostate cancer cells. Int. J. Cancer, *82:* 846 – 852, 1999.

20. Jansen, B., Schalgbauer-Wadl, H., Brown, B. D., Bryan, R. N., van Elsas, A., Muller, M., Wolff, K., Eichler, H.G., and Pehamberger, H. Bcl-2 antisense therapy chemosensitizes human melanoma in SCID mice. Nat. Med., *4:* 232 – 234, 1998.

21. Jansen, B., Wacheck, V., Heere-Ress, E., Schalgbauer-Wadl, H., Hoeller, C., Lucas, T., Hoermann, M., Hollenstein, U., Wolff, K., and Pehamberger, H. Chemosensitization of malignant melanoma by BCL2 antisense therapy. Lancet, *356:* 1728 – 1733, 2000.

22. Kitada, S., Miyashita, T., Tanaka, S., and Reed, J. C. Investigations of antisense oligonucleotides targeted against *bcl*-2 RNAs. Antisense Res. Dev., *3:* 157 – 169, 1993.

23. Stein, C. A. and Cheng, Y. C. Antisense oligonucleotides as therapeutic agents—is the bullet really magical? Science, *261:* 1004 – 1012, 1993.

24. Dias, N. and Stein, CA. The use of antisense oligonucleotides to validate gene function. Mol. Cancer Ther., *1:* 347 – 355, 2001.

25. Chi, K., Wallis, A. E., Lee, C. H., De Menezes, D. L., Sartor, J., Dragowska, W. H., and Mayer, L. D. Effects of Bcl-2 modulation with G3139 antisense oligonucleotide on human breast cancer cells are independent of inherent Bcl-2 protein expression. Breast Cancer Res. Treat., *63:* 199 – 212, 2000.

26. Miyake, H., Hanada, N., Nakamura, H., Kagawa, S., Fujiwara, T., Hara, I., Eto, H., Gohji, K., Arakawa, S., Kamidono, S., and Saya, H. Overexpression of Bcl-2 in bladder cancer cells inhibits apoptosis induced by cisplatin and adenoviral-mediated p53 gene transfer. Oncogene, *16:* 933 – 943, 1998.

27. Miyake, H., Tolcher, A., and Gleave, M. E. Chemosensitization and delayed androgen-independent recurrence of prostate cancer with the use of antisense Bcl-2 oligodeoxynucleotides. J. Natl. Cancer Inst., *92:* 34 – 41, 2000.

28. Guvakova, M. A., Yakubov, L. A., Vlodavsky, I., Tonkinson, J. L., and Stein, C. A. Phosphorothioate oligodeoxynucleotides bind to basic fibroblast growth factor, inhibit its binding to cell surface receptors, and remove it from low affinity binding sites on extracellular matrix. J. Biol. Chem., *270:* 2620 – 2627, 1995.

29. Khaled, Z., Benimetskaya, L., Zeltser, R., Khan, T., Sharma, H. W., Narayanan, R., and Stein, C. A. Multiple mechanisms may contribute to the cellular anti-adhesive effects of phosphorothioate oligodeoxynucleotides. Nucleic Acids Res., *24:* 737 – 745, 1996.

30. Benimetskaya, L., Miller, P., Benimetsky, S., Maciaszek, A., Guga, P., Beaucage, S. L., Wilk, A., Grajkowski, A., Halperin, A. L., and Stein, C. A. Inhibition of potentially anti-apoptotic proteins by antisense protein kinase C-α (Isis 3521) and antisense *bcl-2* (G3139) phosphorothioate oligonucleotides: relationship to the decreased viability of T24 Bladder and PC3 prostate cancer cells. Mol. Pharmacol., *60:* 1296 – 1307, 2001.

31. Tarpey, M. M. and Fridovich, I. Methods of detection of vascular reactive species: nitric oxide, superoxide, hydrogen peroxide, and peroxynitrite. Circ. Res., *89:* 224 – 236, 2001.

32. Yarborough, A., Zhang, Y. J., Hsu, T. M., and Santella, R. M. Immunoperoxidase detection of 8-hydroxydeoxyguanosine in aflatoxin B1 treated rat liver and human oral mucosal cells. Cancer Res., *56:* 683 – 688, 1996.

33. Pani, G., Colavitti, R., Bedogni, B., Anzevino, R., Borrelo, S., and Galeotti, T. A redox signaling mechanism for density-dependent inhibition of cell growth. J. Biol. Chem., *275:* 38891 – 38899, 2000.

34. Gewirtz, A. M., Anfossi, G., Venturelli, D., Valpreda, S., Sims, R., and Calabretta, B. G_1-S transition in normal human T-lymphocytes requires the nuclear protein encoded by c-*myb*. Science, *245:* 180 – 183, 1989.

35. Simbulan-Rosenthal, C. M., Rosenthal, D. S., Luo, R., and Smulson, M. E. Poly(ADP-ribose) polymerase upregulates E2F-1 promoter activity and DNA pol α expression during early S phase, Oncogene. *18:* 5015 – 5023, 1999.

36. Hartman, G., Weeratna, R. D., Ballas, Z. K., Payette, P., Blackwell, S., Suparto, I., Rasmussen, W. L., Waldschmidt, M., Sajuthi, D., Purcell, R. H., Davis, H. L., and Kreig, A. M. Delineation of a CpG phosphorothioate oligodeoxynucleotide for activating primate immune responses *in vitro* and *in vivo*. J. Immunol., *164:* 1617 – 1624, 2000.